J|A|C|S
COMMUNICATIONS

Published on Web 04/27/2006

A Tetracoordinated Rhodium Aminyl Radical Complex

Pascal Maire,[†] Martin Königsmann,[†] Anandaram Sreekanth,[†] Jeffrey Harmer,*[,‡] Arthur Schweiger,[‡] and Hansjörg Grützmacher*[,†]

Laboratory of Inorganic Chemistry, Department of Chemistry and Applied Biosciences, ETH-Zürich, CH-8093 Zürich, Switzerland, and Laboratory of Physical Chemistry, Department of Chemistry and Applied Biosciences, ETH-Zürich, CH-8093 Zürich, Switzerland

Received March 3, 2006; E-mail: gruetzmacher@inorg.chem.ethz.ch; harmer@phys.chem.ethz.ch

Simple aminyl radicals, $R_2N^{\bullet}$, are highly reactive species with lifetimes in the micro- to millisecond range.[1] Relatively persistent aminyls **I** are obtained when the spin density is delocalized in a conjugated π-system and/or an adjacent donor group Y with a lone electron pair in a π-type orbital is bonded to the formally electron-deficient nitrogen atom. When sufficiently bulky substituents are introduced, aminyls can be isolated,[2] and the 2,2-diphenyl-1-picrylhydrazyl (DPPH, R = NO_2, Y = NPh_2)[3] is a prominent example of this strategy (Chart 1). Electron-rich transition metal fragments [M] should be likewise efficient as stabilizing groups. Among those, d^8-Rh(I) containing fragments are especially suited because the metal serves as an electron donor via one of the filled d_{xy}, d_{xz}, or d_{yz}-type orbitals. In addition, the hyperfine coupling of the ^{103}Rh nucleus ($I = {}^1/_2$, 100% natural abundance) allows the spin density on the metal center to be easily detected. Limiting resonance forms to the electronic ground state of an aminyl radical complex are $[M]^{n+}-N^{\bullet}R_2$ **IIa** or $[M]^{(n+1)+}-N^{-}R_2$ **IIb**. In most cases, the metal amide form **IIb** is the better description, that is, the unpaired electron is mainly localized at the metal center.[4a,b] Complexes with the spin density predominantly localized at the nitrogen center as in **IIa** are rare.[4c,d,5]

We demonstrated that the cationic complex $[Rh(trop_2N^{\bullet})(bipy)]^+$ (Chart 1) is best described as an aminyl radical complex in which 57% of the spin population is located on the N and 30% on the Rh center.[5] This trigonal bipyramidal complex contains a coordinatively saturated Rh center with a formal 18-electron configuration. Can an aminyl radical be stabilized by an adjacent tetracoordinated formally 16-electron Rh(I) fragment? This question initiated the experiments reported here.

When the cationic 16-electron Rh(I) diamino complex [Rh(trop$_2$-dach)]OTf **1**[6] [trop$_2$dach = (*R*,*R*)-*N*,*N*′-bis(5*H*-dibenzo[*a*,*d*]cyclohepten-5-yl)-1,2-diaminocyclohexane] is reacted in THF with slightly more than 2 equiv of KO*t*Bu, the diamido rhodate **2** is obtained in a clean reaction (Scheme 1). Crystallization in the presence of 18-crown-6 gave deep green highly air-sensitive crystals of the composition {[K(18C6)(THF)][Rh(trop$_2$dach-2H)]} which were investigated by X-ray diffractions (trop$_2$dach-2H denotes the 2-fold deprotonated ligand). The result is presented in Figure 1, selected bond lengths [Å] and angles [°] are given in the figure caption.

As in the related complex {[K(18C6)(THF)][Rh(trop$_2$dpen)]}[7] [trop$_2$dpen = (*S*,*S*)-*N*,*N*′-bis(5*H*-dibenzo[*a*,*d*]cyclohepten-5-yl)-1,2-diphenyl-1,2-ethylenediamine], **2** forms a loose ion pair in the solid state in which the $[K(18C6)(THF)]^+$ cation binds at about 3.2 Å in a η^2-fashion to one benzo group from the inside of the anion (in {[K(18C6)(THF)][Rh(trop$_2$dpen)]} binding from the outer side is observed).

Chart 1. Concepts to Stabilize Aminyl Radicals

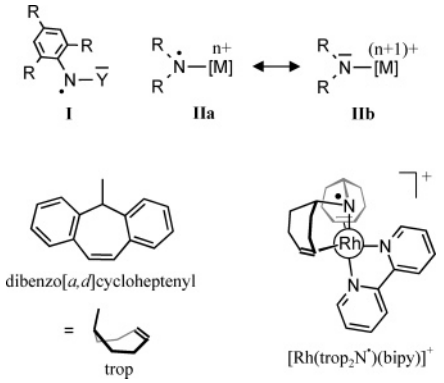

Scheme 1. Synthesis and Reactivity of [Rh(trop$_2$dach)] **3**[a]

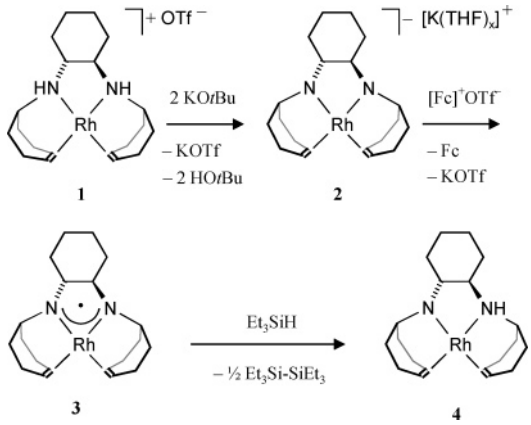

[a] The benzo groups of the trop units in the ligand have been omitted for clarity.

The Rh−N bonds (average 1.993 Å) are slightly shorter than those in the diamino complex **1** (2.095 Å), which seems to be a general feature of amido complexes despite the fact that the interaction of the lone pairs at the N centers and the filled d_{xz} and d_{yz} orbitals at the metal center is antibonding. The sum of bond angles around the N centers (345.7−353.8°) in the diamido complex {[K(18C6)(THF)][Rh(trop$_2$dach-2H)]} is about 10° larger than that in the diamino complex **1** [$\Sigma°$(N) = 340°; H not included].

The deep green color (λ_{max} = 617 nm) of solutions of {[K(18C6)-(THF)][Rh(trop$_2$dach-2H)]} or **2** in DMSO indicates the formation of solvent separated ions, while THF solutions of **2** are red (λ_{max} = 558 nm) which as we believe characterizes intimate host−guest ion pairs in which a partially solvated $[K(THF)_x]^+$ cation is embedded within the anion.[7]

A cyclic voltammogram of **2** in a DMSO/0.1 M nBu$_4$NPF$_6$ electrolyte shows two reversible redox waves at −1.02 and

[†] Laboratory of Inorganic Chemistry.
[‡] Laboratory of Physical Chemistry.

10.1021/ja0612798 CCC: $33.50

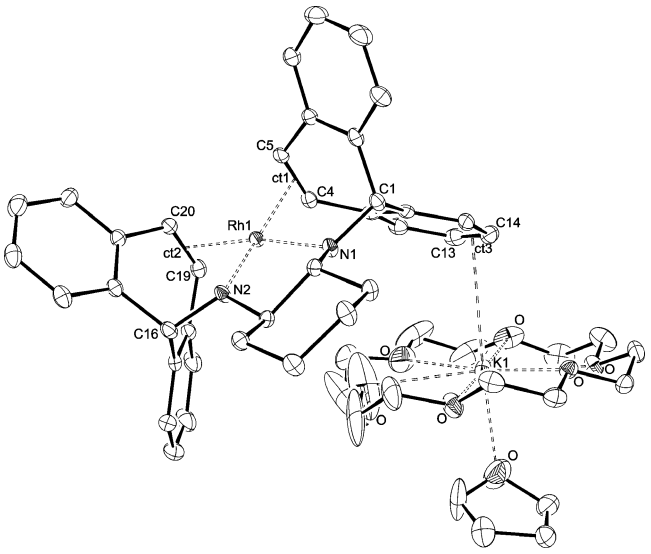

Figure 1. Structure of one of the two independent molecules in {[K(18C6)(THF)][Rh(trop$_2$dach-2H)]}. Hydrogen atoms are omitted for clarity. Thermal ellipsoids are drawn at 30% probability. Selected bond lengths [Å] and angles [°] (data for the second molecule are given in italics): Rh1−N1 1.974(1), Rh1−N2 2.007(2), *Rh2−N3 1.993(1)*, *Rh2−N4 1.997(9)*, Rh1−C4 2.137(6), Rh1−C5 2.121(1), *Rh2−C53 2.126(3)*, *Rh2−C54 2.147(3)*, Rh1−C19 2.148(4), Rh1−C20 2.133(9), *Rh2−C68 2.128(7)*, *Rh2−C69 2.149(3)*, Rh1−ct1 2.006(6), Rh1−ct2 2.023(6), *Rh2−ct4 2.013(3)*, *Rh2−ct5 2.015(3)*, C4═C5$_{trop}$ 1.424(8), C19═C20$_{trop}$ 1.401(8), *C53═54$_{trop}$ 1.433(3)*, *C68═C69$_{trop}$ 1.435(6)*, K1−ct3 3.212(5), *K2−ct6 3.230(5)*, K1−O$_{(18C6)}$ 2.679(2)−2.897(1), *K2−O$_{(18C6)}$ 2.740(2)−2.814(1)*, N1−Rh1−N2 80.9(4), *N3−Rh2−N4 81.1(4)*, N1−Rh1−ct1 90.9(3), N2−Rh1−ct2 91.6(2), *N3−Rh2−ct4 91.5(4)*, *N4−Rh2−ct5 91.8(5)*, ct1−Rh1−ct2 97.3(7), *ct4−Rh2−ct5 97.5(2)*; φ = 9.8°, *φ = 15.1°* (ct = centroids of C═C bonds; φ is the intersection of the planes spanned by the rhodium atom, the N atom and ct of each bischelate ligand).

−0.38 V vs the Fc$^+$/Fc couple (T = 293 K, scan rate = 100 mV s^{-1}, Pt-working electrode). Especially the first oxidation step [Rh(trop$_2$dach-2H)]$^-$ (**2**) → [Rh(trop$_2$dach-2H)]$^\bullet$ (**3**) + e$^-$ at $E^{\circ 1}{}_{ox}$ = −1.02 V occurs at a remarkable low potential compared to related rhodium monoamido complexes (E°_{ox} = −0.5 to −0.3 V).[5−7] The stability of the radical [Rh(trop$_2$dach-2H)]$^\bullet$ (**3**) is sufficient to allow its preparation by oxidation of **2** with ferrocenium triflate, [Fc]$^+$OTf$^-$. The neutral complex **3** could be isolated by rapid workup as a deep red microcrystalline powder, but attempts to grow larger crystals failed because **3** reacts with the solvent, whereby the amino amido complex **4**[6] was formed in high yield.

Like [Rh(trop$_2$N$^\bullet$)(bipy)]$^+$, the complex **3** undergoes fast hydrogen abstraction reactions with nBu$_3$SnH [BDE(Sn−H) = 308.5 kJ mol^{-1}] or PhSH [BDE(S−H) = 348.7 kJ mol^{-1}] which both have lower element hydrogen bond dissociation energies (BDE) than the estimated N−H bond dissociation energy in **4** (360 kJ mol^{-1}).[5,6] Phenol, with a higher BDE(O−H) = 376 kJ mol^{-1}, does not react with **3**. The silane, Et$_3$SiH with BDE(Si−H) = 356 kJ mol^{-1}, does not react with [Rh(trop$_2$N$^\bullet$)(bipy)]$^+$. However, **3** reacts within a few minutes quantitatively with Et$_3$SiH to give disilane Et$_3$Si−SiEt$_3$ and **4**, which was obtained in high yield in all reactions reported here. This shows that the tetracoordinated [Rh(trop$_2$dach-2H)]$^\bullet$ (**3**) is more reactive than the pentacoordinated aminyl radical complex [Rh(trop$_2$N$^\bullet$)(bipy)]$^+$.

This reactivity indicated that a significant part of the spin density in **3** may be localized on the N-centers. This assumption is fully supported by CW and pulse EPR spectroscopy[8] in combination with DFT calculations.[9]

The X-band CW-EPR spectrum of **3** in diethyl ether measured at 298 K is shown in Figure 2A. The spectrum is well resolved

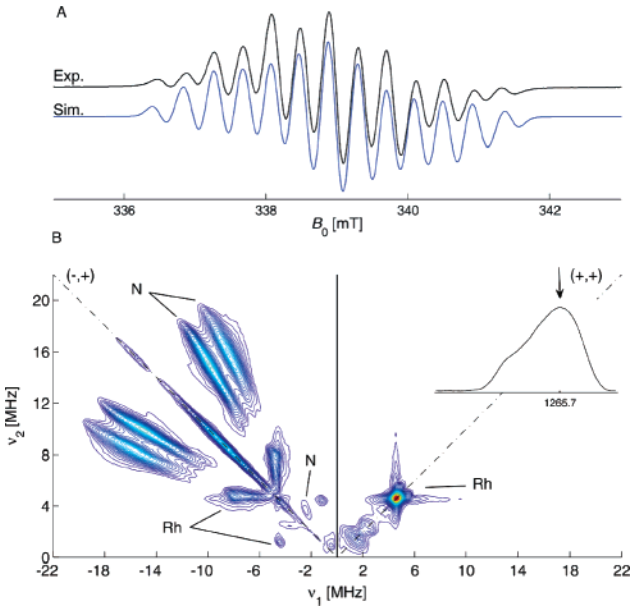

Figure 2. EPR of **3** in diethyl ether. (A) X-band CW-EPR spectrum measured at 298 K. Experiment (Exp.), simulation (Sim.). (B) Q-band matched-HYSCORE spectrum measured at 25 K, near to the g_2 observer position (see inset). Cross-peaks from ^{103}Rh and ^{14}N are labeled.

Table 1. EPR Parameters and Spin Populations, ρ, of Compound **3**. DFT Values are Given in Brackets. The Signs of the Experimental Hyperfine Interactions Are Assigned According to the DFT Results

g_{iso} = 1.9963 ± 3, g_1 = 2.005 ± 1, g_2 = 1.992 ± 1, g_3 = 1.991 ± 1				
	ρ	A_1, A_2, A_3 (MHz)	A_{iso} (MHz)[b]	T_1, T_2, T_3 (MHz)[b]
^{103}Rh		6.0, 4.6, −13.3[c]	−0.7	6.9, 5.5, −12.6
	(41%)	(−44.4, −47.0, −79.0)	(−56.8)	(12.4, 9.7, −22.2)
^{14}N[a]	24% × 2	−1.9, −1.9, 37.0[d]	11.1	−12.9, −12.9, 25.9
	(28% × 2)	(−0.9, −0.8, 37.6)	(12.0)	(−12.9, −12.7, 25.7)
^{1}H$_\beta$	2.3% × 2	27.1, 29.3, 34.5[d]	32.6	−3.2, −1.0, 4.2
	(2.8% × 2)	(52.6, 54.7, 59.6)	(55.7)	(−3.1, −0.9, 4.0)
^{1}H$_{bz}$	1.0% × 2	11.5, 14.5, 19.0[c]	14.3	−3.5, −0.5, 4.0
	(1.0% × 2)	(4.0, 4.4, 10.9)	(6.4)	(−2.4, −2.0, 4.5)

[a] The nuclear quadrupole parameters are $\kappa = e^2qQ/h$ = 2.2 MHz and η = 1. DFT gives κ = 2.7 MHz, η = 0.9. [b] Isotropic part of the hyperfine interaction, $A_{iso} = (A_1 + A_2 + A_3)/3$, dipolar part of the hyperfine interaction, $(T_1, T_2, T_3) = (A_1 - A_{iso}, A_2 - A_{iso}, A_3 - A_{iso})$. [c] Estimated errors ±0.5 MHz. [d] Estimated errors ±1 MHz.

and yields after simulation the isotropic hyperfine couplings attributed to aminyl N, H$_\beta$, and H$_{bz}$ nuclei (Table 1). Measurements made on frozen solutions of **3** enabled the anisotropic parts of the EPR parameters to be determined. The principal g values were obtained from a field-swept EPR spectrum recorded at Q-band (Figure S1). Pulse ENDOR (electron nuclear double resonance) and HYSCORE (hyperfine sublevel correlation) spectroscopy were used to determine the hyperfine parameters of Rh, N (Figures 2B and S4), and H$_\beta$ and H$_{bz}$ (Figures S2 and S3). The complete set of experimentally derived parameters is given in Table 1, along with the data calculated by DFT. Experimental spin populations were estimated from the hyperfine couplings.[10] The experimental and calculated hyperfine couplings of the aminyl nitrogens are in good agreement and support the ∼50% spin population. The dipolar parts of the hyperfine interactions, T, of the two hydrogen nuclei are sensitive to the spin density distribution, and the satisfactory agreement between experiment and calculation is in support of this distribution (Figure 3).

In particular, the small T for the two protons H$_\beta$ indicates that there is negligible spin density on the C$_\beta$. The isotropic parts, A_{iso},

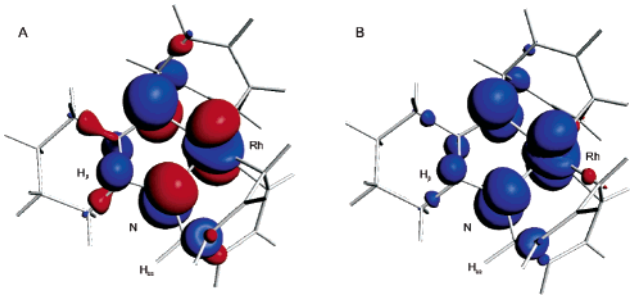

Figure 3. Plot of (A) singly occupied molecular orbital, and (B) the spin density distribution (blue positive, red negative) of [Rh(cht$_2$dach)]. Selected computed structural data: Rh−N 1.986 Å, Rh−ct 2.075 Å, C═C$_{cht}$ 1.445 Å; N−Rh−N 82.8°, ct−Rh−ct 97.4°, N−Rh−ct 92.4°; ct = centroid of the coordinated C═C bond.

Chart 2. Spherically Delocalized Noninnocent Ligand Complex **A** and Centrally Metal Delocalized Radical Complex **B**

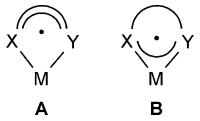

are largely due to spin polarization[11] and are not modeled accurately by the DFT calculation. For rhodium, the calculated dipolar part of the hyperfine interaction is in reasonable agreement with the experimental value, whereas the isotropic component is unreliable. Calculation of transition metal hyperfine couplings is notoriously inaccurate because of the difficulty to correctly calculate spin polarization effects.[12] The anisotropy of the *g* values is small in comparison to that of typical Rh(II) complexes, which may indicate that the spin population on the rhodium is overestimated by the calculation.

Figure 2B shows a representative HYSCORE spectrum that contains both nitrogen and rhodium signals. The long ridges assigned to nitrogen result from the large anisotropy in the hyperfine interaction, and their splitting into two sets is the result of the nuclear quadrupole interaction. Signals from rhodium form part of a cross, with the splittings at the edges allowing the principal values of the nearly axial hyperfine interaction to be evaluated.

According to the DFT calculations with the model compound [Rh(cht$_2$dach)] (cht = cycloheptatrienyl; see Figure 3), the main part of the spin population is located on the two aminyl nitrogens (28% × 2) and the rhodium center (41%). This can be seen by inspection of Figure 3, which shows the singly occupied molecular orbital and spin density.

In contrast to the well-studied complexes **A** with "noninnocent" ligands X ∩ Y,[13] where the unpaired electron is delocalized in the conjugated ligand sphere, the situation in **3** is different and the unpaired electron is centrally delocalized over the metal center (Chart 2). Both concepts allow the synthesis of rather persistent metal-coordinated radicals.

Acknowledgment. This work was supported by the ETH and the Swiss National Science Foundation. We thank the reviewers for their remarks.

Supporting Information Available: Detailed experimental and structural data and EPR spectroscopy containing Figures S1−S4. This material is available free of charge via the Internet at http://pubs.acs.org.

References

(1) (a) Merényi, G.; Lind, J. In *N-centered Radicals*; Alfassi, Z., Ed.; Wiley: New York, 1998; pp 599−613. (b) Maxwell, B. J.; Tsanaktsidis, J. In *N-centered Radicals*; Alfassi, Z., Ed.; Wiley: New York, 1998; pp 663−684.

(2) (a) Miura, Y.; Tomimura, T. *Chem. Commun.* **2001**, 627. (b) Miura, Y.; Tomimura, T.; Teki, Y. *J. Org. Chem.* **2000**, *65*, 7889−7895.

(3) Williams, D. E. *J. Am. Chem. Soc.* **1966**, *88*, 5665−5666.

(4) (a) For a Ru(III) amido complex with 8% spin density on N, see: Ingleson, M. J.; Pink, M.; Huffman, J. C.; Fan, H.; Caulton, K. G. *Organometallics* **2006**, *25*, 1112−1119. (b) Kaim, W.; Gross, R. *Angew. Chem., Int. Ed. Engl.* **1985**, *24*, 856. (c) Co(III) and Mn(IV) anilinyl radical complexes: Penkert, F. N.; Weyhermüller, T.; Bill, E.; Hildebrandt, P.; Lecomte, S.; Wieghardt K. *J. Am. Chem. Soc.* **2000**, *122*, 9663−9673. (d) For a related β-diketiminate Ni(III) iminyl radical complex with 57% spin density on the N, see: Kogut, E.; Wiencko, H. L.; Zhang, L.; Cordeau, D. E.; Warren, T. H. *J. Am. Chem. Soc.* **2005**, *127*, 11248−11249.

(5) Büttner, T.; Geier, J.; Frison, G.; Harmer, J.; Calle, C.; Schweiger, A.; Schönberg, H.; Grützmacher, H. *Science* **2005**, *307*, 235−238.

(6) Maire, P.; Breher, F.; Schönberg H.; Grützmacher, H. *Organometallics* **2005**, *24*, 3207−3218.

(7) Maire, P.; Breher, F.; Grützmacher, H. *Angew. Chem., Int. Ed.* **2005**, *44*, 6325−6329.

(8) Schweiger, A.; Jeschke, G. *Principles of Pulse Electron Paramagnetic Resonance*; Oxford Press: Oxford, 2001.

(9) Density functional theory calculations were performed with the Amsterdam Density Functional (ADF 2005.01) package. Details are given in the Supporting Information.

(10) Morton, J. R.; Preston, K. F. *J. Magn. Reson.* **1978**, *30*, 577−582.

(11) Werst, M. M.; Davoust, C. E.; Hoffman, B. M. *J. Am. Chem. Soc.* **1991**, *113*, 1533−1538.

(12) Munzarová, M. L.; Kubáček, P.; Kaupp, M. *J. Am. Chem. Soc.* **2000**, *122*, 11900−11913.

(13) There is a vast quantity of literature on this topic, which is impossible to provide here; see the selected recent references and literature cited therein: (a) Ray, K.; Weyhermüller, T.; Goossens, A.; Crajé, M. W. J.; Wieghardt, K. *Inorg. Chem.* **2003**, *42*, 4082−4087. (b) Beloglazkina, E. K.; Moiseeva, A. A.; Chizhevskii, A. A.; Tarasevich, B. N.; Zyk, N. V.; Butin, K. P. *Russ. Chem. Bull., Int. Ed.* **2003**, *52*, 1990−2004. (c) See ref 1 in: Breher, F.; Böhler, C.; Frison, G.; Harmer, J.; Liesum, L.; Schweiger, A.; Grützmacher, H. *Chem.—Eur. J.* **2003**, *9*, 3859−3866.

JA0612798